Photonic-Enabled RF Canceller with Tunable Time-Delay Taps

Kenneth E. Kolodziej, Sivasubramaniam Yegnanarayanan, Bradley T. Perry
MIT Lincoln Laboratory
Lexington, Massachusetts, USA

***Abstract*—Future 5G wireless networks can benefit from the use of in-band full-duplex technologies that allow access to previously unused spectrum by suppressing consequential self-interference. While this interference mitigation is typically achieved using multiple techniques, existing RF cancellation schemes can limit a system's center frequency and instantaneous bandwidth. This paper introduces a unique RF canceller design that uses photonics and a vector modulator architecture to provide a high number of canceller taps with tunable time-delays, which allow the canceller to operate over wide bandwidths. A prototype of this concept was built, and successfully demonstrated the capability of tuning 20 canceller taps over 80 different delay locations that spanned 115 ns.**

***Index Terms*—5G mobile communication, in-band full-duplex, interference cancellation, microwave photonics, RF cancellation.**

I. Introduction

In-Band Full-Duplex (IBFD) technologies are being considered for 5th generation (5G) wireless systems to increase both user and data capacity by improving spectral efficiency over existing networks. The main challenge of implementing these systems is overcoming the self-interference (SI) that occurs when transmitting and receiving during the same timeslot on a given frequency band. By reducing this SI in the analog domain, before the receiver's low-noise amplifier (LNA), saturation can be avoided and spurious signals minimized in order to maintain the receiver's dynamic range. Many IBFD systems include an RF canceller for this purpose, and typically utilize it in conjunction with one or more antenna isolation-improving techniques to mitigate SI at the input of a receiver.

Previously published RF cancellers have been shown to provide sufficient SI cancellation, but are limited to fixed center frequencies and narrow instantaneous bandwidths, less than 120 MHz centered at 2.45 GHz [1]–[3]. While the center frequency is dictated by the RF components selected, the bandwidth constraint fundamentally stems from two main sources. First, RF cancellers with tapped-delay line architectures can only have a limited number of taps due to the significant losses incurred by both splitting and combining the signal. Second, the delay spread, the difference between the maximum and minimum tap delays, is small due to the fact that the delays are implemented using coaxial cables where the physical lengths and propagation losses are unmanageable for many systems. These drawbacks reduce a canceller's ability to adapt to a diverse set of interference channels, which restricts its usefulness in different applications, but can be overcome by incorporating photonic components into the design.

Distribution A: approved for public release; unlimited distribution. This material is based upon work supported under Air Force Contract No. FA8721-05-C-0002 and/or FA8702-15-D-0001. Any opinions, findings, conclusions or recommendations expressed in this material are those of the author(s) and do not necessarily reflect the views of the U.S. Air Force.

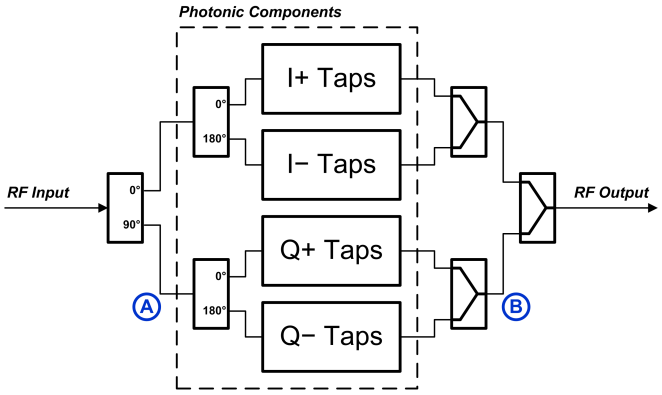

Fig. 1. RF canceller block diagram highlighting the photonic components and vector modulator architecture.

The use of photonics for IBFD applications has initially been researched, but was limited to a circulator-type device for single-antenna systems [4] and a single-tap canceller that can inherently only process narrowband signals [5]. This paper introduces a novel RF canceller architecture that is based on the use of photonic components to achieve both a high number of taps with tunable time-delays and a high delay spread with minimal insertion loss. This is the first known system to provide a practical path towards cancelling signals over wide instantaneous bandwidths, up to 1 GHz, and over a significant range of center frequencies, from 1 to 6 GHz.

The design of the photonic-enabled RF canceller is described in Section II, while the results of our initial measurements are presented in Section III. Conclusions are derived in Section IV.

II. Canceller Description

A. Vector Modulator Architecture

The basic block diagram of the photonic-enabled RF canceller is shown in Fig. 1. This diagram illustrates the canceller's vector modulator architecture using tapped delay lines, and highlights the functional blocks that were implemented as photonic components in our design. Vector modulators can simultaneously adjust the phase and amplitude of a signal after splitting it into in-phase (I) and quadrature (Q) channels. Each of these channels can then be split again into two signals that are 180 degrees apart, which produces a total of four

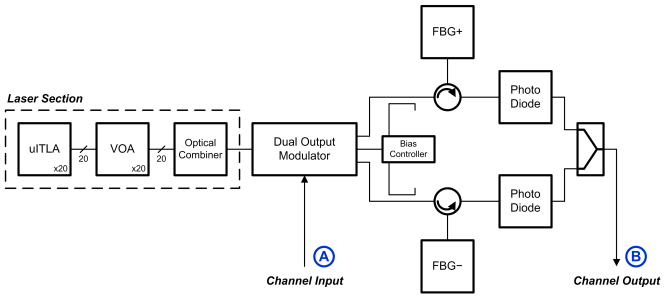

Fig. 2. Component diagram of the identical I and Q canceller channels.

signals, or vectors, with phase shifts of 0 (I+), 90 (Q+), 180 (I−) and 270 (Q−) degrees. These four signals are then individually adjusted in amplitude and combined in-phase, which allows the vector modulator to effectively produce arbitrary amplitudes and phase shifts of the input. As seen in Fig. 1, the 180-degree phase shifts as well as the positive and negative taps for both I and Q channels were realized using photonic elements. These I/Q channels are identical, and referenced in the diagram with inputs (A) and outputs (B).

The impulse response of this tapped delay line vector modulator can be expressed as the combination of the individual contributions from the four tap blocks, as shown in

$$h_{canc}(t) = (h_{I+Taps}(t) - h_{I-Taps}(t)) + e^{-j\frac{\pi}{2}}\,(h_{Q+Taps}(t) - h_{Q-Taps}(t)) \quad (1)$$

This equation assumes that the input splitters provide ideal phase shifts without any amplitude differences, and that there is no phase or amplitude imbalance in the combining network after the taps. These photonic-based taps are the core of the RF canceller, and their design will be discussed in the next subsection.

B. Detailed Design

The detailed block diagram for the identical I/Q channels is shown in Fig. 2, and carries over the input and output labels from Fig. 1 for orientation. The left side of the diagram shows the laser section that generates multiple optical carriers, which will be translated into RF canceller taps, as will be described below. These optical carriers were implemented using micro integrable tunable laser assemblies (uITLA) that contain a CW-tunable laser in a compact form factor. We selected uITLAs from Emcore since they were capable of tuning over the entire optical communications C-band, 191.50 to 196.25 THz, and had +10 dBm of output power. Our initial design utilized 20 such lasers, which resulted in 20 RF canceller taps, but is not limited to this number.

Following each of the uITLAs is a variable optical attenuator (VOA), which can adjust the laser's power level. A polarization-maintaining (PM) micro-electro-mechanical system (MEMS) attenuator from DiCon Fiberoptics was utilized, and provided 30 dB of optical attenuation range, which translates to 60 dB of RF attenuation. This device was controlled using a DC drive voltage that was generated from a digital-to-analog converter (DAC), which was configured using an FPGA. The last component in the laser section is a PM optical combiner that sums the 20 optical carriers after they have been individually attenuated by their respective VOAs. For this function, we selected a 32-channel passive combiner from Enablence Technologies.

For both I/Q channels, the output of the laser section is a single fiber containing 20 CW optical carriers that can be tuned in frequency, over 191.50 to 196.25 THz, and amplitude with up to 30 dB of attenuation. These carriers are used to drive a Lithium Niobate Mach-Zehnder Modulator with dual outputs that are phased 180 degrees apart, and effectively implement the 180-degree functional blocks shown in Fig. 1. A custom low-loss, low-V_π modulator from EOSPACE was chosen, and was specified with an RF bandwidth of DC to 6 GHz, which establishes the wide range center frequencies for the overall RF canceller. This RF input to the modulator, labeled Channel Input and denoted as A in Fig. 2, is effectively up-converted on to the 20 optical carriers driving the modulator. Both outputs of the modulator are coupled off using 1% optical couplers and supplied to a bias controller that was responsible for maintaining an optimal bias point for both bandwidth and linearity.

These modulated outputs are then connected to separate Fiber Bragg Gratings (FBG) through optical circulators. FBGs are special fibers that are designed to reflect specific frequencies by changing the refractive index at certain distances along the fiber's core. These refraction changes are typically referred to as taps. Since the taps, and subsequent signal reflections, are deliberately inscribed into the fiber, the distances at which they occur can be translated into corresponding time delays that are dependent on the chosen optical frequencies. For example, an FBG could be designed to reflect two signals with frequencies, f_1 and f_2, at distances of 0.3 and 0.6 meters, respectively. If propagation in the fiber is assumed to be at the speed of light, the delay for f_1 would be 2.0 ns and the delay for f_2 would be 4.0 ns based on the simple equation, $delay = \frac{2d}{c}$, where d is the distance to each refraction point and c is the speed of light.

The canceller design utilized two custom FBGs with 80 taps each that covered 192 to 196 THz with 50 GHz of spacing and 1.3 ns of delay between adjacent taps. As shown in Fig. 2, the 0-degree modulator output was connected to FBG+, and the 180-degree output was connected to FBG−, which are unique FBGs with different starting frequencies for the 80 taps. By selecting different frequency values for the positive and negative taps, a single laser could be used to tune to either of them (since only one is used at a given time) instead of requiring two lasers. The first tap of FBG+ was centered at 196.075 THz, while the first tap for FBG− was centered at 196.050 THz. The FBG tap number, n, can then be determined based on the optical carrier frequency, f_c , according to

$$n[f_c] = \frac{f_1 - f_c}{f_{spacing}} + 1, \quad (2)$$

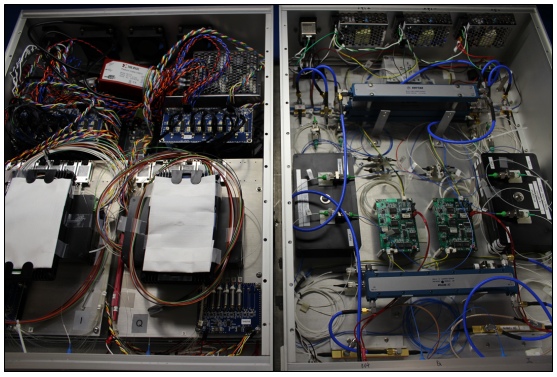

Fig. 3. Photonic-enabled RF canceller prototype system.

where f_1 is the frequency corresponding to the first tap of the FBG, and $f_{spacing}$ is the 0.050 THz spacing between taps. Eq. 2 assumes that f_c is offset from f_1 by an integer multiple of $f_{spacing}$ since the taps are at discrete locations.

The FBGs were fabricated with 8 taps inscribed into a section of fiber that was 1 meter long, and then 10 of these sections were spliced together for a total length of 10 meters. Due to the limitations of the splicing equipment, an additional delay of 1.3 ns was inserted between fiber sections. The tap-dependent time delay in nanoseconds along the fiber is described by

$$\tau[n] = 1.3\left(n + floor\left(\frac{n-1}{8}\right)\right), \tag{3}$$

where n is the discrete tap index between 1 and 80, and the $floor$ term is added to account for the splice delays that occur after ever 8 taps. The baseband-equivalent impulse response of the identical tap sections can then be formulated as the sum of K optical carriers, as shown in

$$h_{Taps}(t) = \sum_{k=1}^{K} \alpha_k \delta\left(t - \tau_k\left[f_c\right]\right), \tag{4}$$

where every carrier is attenuated by α_k from its VOA and delayed by an amount that is dependent on the carrier frequency, f_c, which is dictated by the FBG design. This equation can be substituted into Eq. 1 to provide the complete tuning representation for the vector modulator canceller architecture. While Eq. 4 ignores the optical modulation/demodulation effects and RF losses, it highlights the tunable-delay capability of the canceller taps, which is unique to this design.

Finally, optical circulators are used to direct the time-delayed reflected signals to the photodiodes, which convert the signals back to RF by removing the optical carriers. The RF signals from these positive and negative taps are then summed using an in-phase combiner, and combined again between the I and Q channels, as illustrated in Fig. 1. The resulting RF output is a modified version of input signal that has been adjusted in amplitude using the VOAs and delayed in time using the FBGs to match the SI channel.

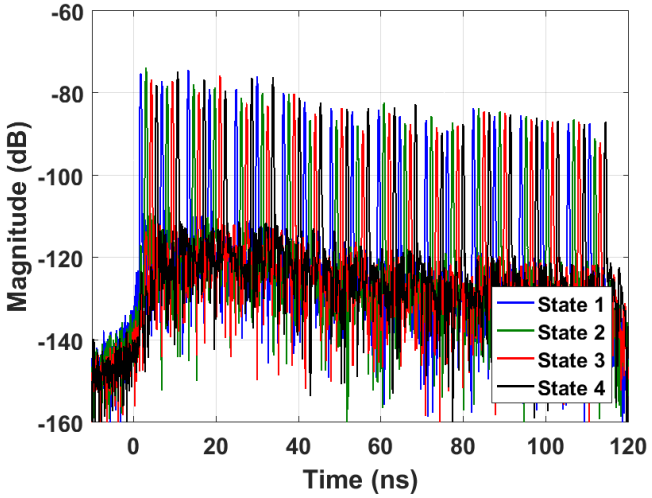

Fig. 4. Time-domain transmission response of the canceller showing 80 tunable delay locations by moving 20 active taps through four different states.

C. Prototype System

A prototype has been developed to demonstrate this canceller concept, and was housed in two 4U rack-mount chassis as shown in Fig. 3. The chassis on the left contains all of the components in the laser section, which is referenced in Fig. 2, for both I and Q channels. It therefore has 40 lasers connected to 40 VOAs, two optical combiners, control circuitry and necessary power supplies. The rightmost chassis encloses all of the other photonic components as well as the RF splitters and combiners. It should be noted that during the design of this prototype, minimal effort was made to reduce its volume, but it could certainly be miniaturized in the future with the use of custom photonic integrated circuits.

III. Results

The canceller prototype was evaluated in the laboratory using an Agilent Technologies' N5222A network analyzer connected to the RF input and output ports indicated in Fig. 1. The analyzer was configured to sweep 10 MHz to 6 GHz with +10 dBm of output power, and compute the time-domain transmission response (TDT), or effective impulse response, of the system. By investigating the canceller response in the time domain, the functionality and contributions of the individual taps can easily be determined.

The TDT response of the canceller is plotted in Fig. 4. This measurement was configured to evaluate the 0-degree path of the canceller, and therefore tuned the taps in the I+ block shown in Fig. 1. The four different states represented in the figure show four unique measurements where the FBG's starting tap number was changed between 1, 2, 3 and 4 for all 20 lasers. Each state contains 20 delayed responses, and the four states together illustrate all of the 80 possible tap locations within the FBG. It is evident that the delays extend from approximately 0 to 115 ns with 1.3 ns steps, except for the splices after sets of 8 taps, which was expected and described in Eq. 3. The tap losses are slightly high, but can be improved

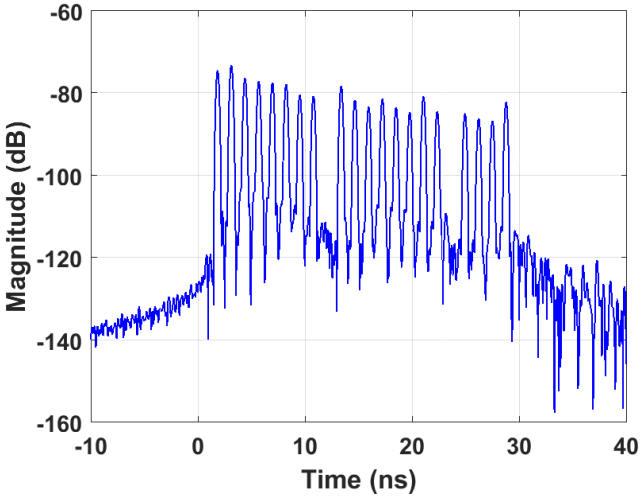

Fig. 5. Time-domain transmission response of the canceller using the first 20 delay locations.

by inserting an optical amplifier after the laser section to compensate for the loss of the passive optical combiner.

The laser frequencies were subsequently tuned to the first 20 delay locations, which resulted in the response shown in Fig. 5, where the different tap and splicing delays are clearly visible. These plots show that the canceller has the ability to tune the delays of 20 active canceller taps over 80 possible delay positions as defined by the FBG design. This presents a significant improvement over previously reported RF cancellers that have fixed delay positions and a maximum tap number of 1 [5], 2 [1], 4 [2] and 16 [3], which limit their overall ability to mitigate SI for wideband signals and multipath-rich environments.

IV. Conclusion

IBFD systems require the mitigation of SI to potentially increase capacity for 5G wireless networks, and typically do this before the receiver's input by using RF cancellation techniques. This SI suppression becomes more challenging for networks that employ wideband signals or operate in environments that exacerbate the multipath effects of the wireless channel. To overcome these challenges, we designed a novel RF canceller architecture that uses photonic components to provide a high number of canceller taps with a wide range of tunable time-delays. A prototype system was constructed to verify this canceller concept, and initial measurements confirmed its ability to successfully tune up to 20 taps over 80 possible delays that covered 115 ns. These results provide a path forward for high-tap count cancellers, and indicate that wideband signal cancellation in multipath-rich environments is possible for future 5G systems with IBFD technology.

Acknowledgment

The authors would like to express their gratitude to Paul Juodawlkis, Rory Fagan, Mark Fosberry and Joseph McMichael for their technical insights; Frederick O'Donnell, Robert Devine and Ryan Maxson for assembling the prototype system; and Ellen Allen and Nicole Shinopulos for their help procuring all of the components.

References

[1] T. Huusari, Y. S. Choi, P. Liikkanen, D. Korpi, S. Talwar, and M. Valkama, "Wideband self-adaptive rf cancellation circuit for full-duplex radio: Operating principle and measurements," in *2015 IEEE 81st Vehicular Technology Conference (VTC Spring)*, pp. 1–7, May 2015.

[2] K. E. Kolodziej, J. G. McMichael, and B. T. Perry, "Multitap rf canceller for in-band full-duplex wireless communications," *IEEE Transactions on Wireless Communications*, vol. 15, pp. 4321–4334, June 2016.

[3] D. Bharadia, E. McMilin, and S. Katti, "Full Duplex Radios," *SIGCOMM Comput. Commun.*, pp. 375–386, Aug 2013.

[4] C. H. Cox and E. I. Ackerman, "Tiprx: A transmit-isolating photonic receiver," *Journal of Lightwave Technology*, vol. 32, pp. 3630–3636, Oct 2014.

[5] M. P. Chang, P. R. Prucnal, and Y. Deng, "Full-duplex spectrum sensing in cognitive radios using optical self-interference cancellation," in *2015 9th International Conference on Sensing Technology (ICST)*, pp. 341–344, Dec 2015.